Journal of Materials Chemistry B

Accepted Manuscript

This is an *Accepted Manuscript*, which has been through the Royal Society of Chemistry peer review process and has been accepted for publication.

Accepted Manuscripts are published online shortly after acceptance, before technical editing, formatting and proof reading. Using this free service, authors can make their results available to the community, in citable form, before we publish the edited article. We will replace this *Accepted Manuscript* with the edited and formatted *Advance Article* as soon as it is available.

You can find more information about *Accepted Manuscripts* in the Information for Authors.

Please note that technical editing may introduce minor changes to the text and/or graphics, which may alter content. The journal's standard Terms & Conditions and the Ethical guidelines still apply. In no event shall the Royal Society of Chemistry be held responsible for any errors or omissions in this *Accepted Manuscript* or any consequences arising from the use of any information it contains.

ROYAL SOCIETY OF CHEMISTRY

www.rsc.org/materialsB

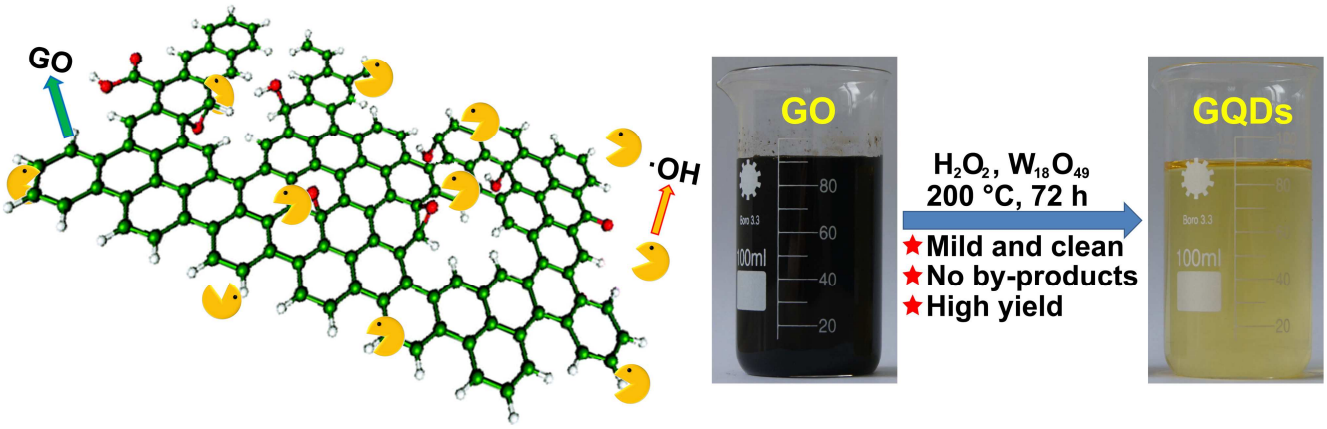

Journal of Materials Chemistry B Accepted Manuscript

Journal Name

COMMUNICATION

A new mild, clean and high-efficient method for preparation of graphene quantum dots without by-products †

Received 00th January 20xx,
Accepted 00th January 20xx

DOI: 10.1039/x0xx00000x

www.rsc.org/

Chong Zhu [a b c †], Siwei Yang [c †], Gang Wang [c], Runwei Mo [c], Peng He [c], Jing Sun [c], Zengfeng Di [c], Zhenhui Kang [d], Ningyi Yuan [a b], Jianning Ding [a b*], Guqiao Ding [c *], Xiaoming Xie [c]

We demonstrated that graphene oxide (GO) can be oxidated and cut into graphene quantum dots (GQDs) by hydroxyl radicals (·OH) which is obtained by catalytic decomposition of hydrogen peroxide (H_2O_2) with tungsten oxide nanowires ($W_{18}O_{49}$) catalyst. The clean oxidizing agent (H_2O_2) and solid catalyst lead to a simple GQD preparing method without any by-products. The obtained GQD aqueous solution can be directly applied to fluorescent imaging in *vitro* without any further purifications. The effect of $W_{18}O_{49}$ catalyst on the ·OH formation is discussed, and the size of GQDs can be controlled via changing the concentration of hydroxyl radicals.

Graphene quantum dots (GQDs), with quantum confinement and edge effects, [1-4] have generated an enormous interests in carbon science and technology due to the unique optical properties, [5-8] biological properties, [5, 9] catalytic performance, [10] semiconducting properties, [11] and electrical properties. [12] Yang *et al.* demonstrated that the chemical structure change of GQDs during modification or reduction suppresses non-radiative recombination of localized electron-hole pairs and/or enhances the integrity of surface π electron network. [13] This process results in a change from the green luminescence to blue luminescence, and the GQDs are successfully applied in near-IR excitation for bioimaging. Hong *et al.* demonstrated that GQDs play an important role in increasing optical absorptivity and charge carrier extraction of the bulk heterojunction solar cells. [14] Moreover, GQDs are also important component section of functional composite materials. [10-12]

By now, the synthetic approaches towards GQDs fall into two broad categories: top-down and bottom-up approaches. [15] Top-down approaches involve the decomposition and exfoliation of cheap, readily available bulk sp^2 carbon materials, most commonly graphite, in harsh conditions. [16, 17] However, most top-down methods (except electrochemical cutting, [18] but this method also always introduced the electrolyte which is also hard to be removed) depend on the powerful oxidants and concentrated acids (such as: $KClO_3$, $KMnO_4$, HNO_3 and H_2SO_4). [19] These oxidants, acids and process are dangerous and pollutional. [20] The most importantly, the by-products in preparation progress, including high concentration inorganic salts and acid residues, result in the fussy and inefficient purification progress (typically dialysis or ultrafiltration centrifugation). [21] This greatly limited the large scale synthesis and application of GQDs. On the other hand, bottom-up approach involves the synthesis of GQDs from polycyclic aromatic compounds or other molecules with aromatic structures. [15, 22, 23] Such approach allows for excellent control of the properties of the final products, however, the complex preparation progress and low yield limited its development and actual applications. [24] Moreover, recently, there are several reports about GQDs bottom-up synthesis using citric acid or other nonaromatic molecules, but general hydrothermal process is hard to obtain well organized sp^2 carbon, and also have some by-products. [25] Thus, it is very significant and important to develop mild, clean and high-efficient method for preparation of GQDs without by-products.

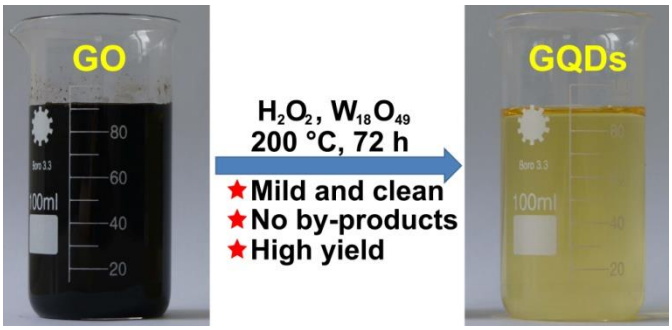

Figure 1 Digital photos of GO aqueous solution (left) and GQD aqueous solution (right). This reaction is catalyzed by $W_{18}O_{49}$ under 200 °C.

[a] Jiangsu Collaborative Innovation Center for Photovolatic Science and Engineering, School of Materials Science and Engineering, Changzhou University, Changzhou, 213164, Jiangsu, China.
[b] Jiangsu Province Cultivation base for State Key Laboratory of Photovoltaic Science and Technology, Changzhou University, Changzhou, 213164, Jiangsu, China.
[c] State Key Laboratory of Functional Materials for Informatics, Shanghai Institute of Microsystem and Information Technology, Chinese Academy of Science, Shanghai, 200500, China.
[d] Institute of Functional Nano & Soft Materials (FUNSOM), Collaborative Innovation Center of Suzhou Nano Science and Technology, Soochow Univeristy, Suzhou, 215123, China.

† Electronic Supplementary Information (ESI) available: [Experimental Section; digital photo, TEM of $W_{18}O_{49}$; digital photo of reaction liquid with and without $W_{18}O_{49}$; XPS, brief summary, stability of GQDs]. See DOI: 10.1039/x0xx00000x

Journal of Materials Chemistry B Accepted Manuscript

Please do not adjust margins

Here, we report the hydrothermal treatment for the mixture of graphene oxide (GO) and H_2O_2 with the tungsten oxide nanowires ($W_{18}O_{49}$) catalyst. The hydroxyl radical (·OH) which is produced from the catalytic decomposition of H_2O_2 can oxidize and cut the GO effectively. The reaction products are only H_2O and GQDs, and the solid $W_{18}O_{49}$ catalyst remains unchanged. Thus, the as-prepared solution can be easily purified by centrifugal separation to remove the catalyst, and the obtained GQD aqueous solution can be directly applied to fluorescent imaging in *vitro* without any further purifications. Moreover, due to the ·OH cutting progress, the size of as-prepared GQDs can be easily controlled via changing the concentration of oxidizing agent.

The preparation process is as follows: $W_{18}O_{49}$ nanowires were obtained by modified method described previously (experimental details, digital photos and characterization are shown in Supporting Information). [26] Typically, 5.0 mL, 30 mg mL^{-1} GO aqueous solution (Figure 1) was added into 5.0 mL, 2.0 M (6 wt. %) H_2O_2 aqueous solution. Then, 50 mg $W_{18}O_{49}$ nanowires were added into this mixture. The obtained mixture was transferred into a 15 mL Teflon®-lined autoclave and heated at 200 °C for 72 h. The pale yellow GQD aqueous solution (Figure 1) can be easily obtained after simple centrifugal separation (to remove the catalyst). It should be emphasized that after hydrothermal treatment the solution is pale yellow, not black, which means that the method is very efficient and all the large GO nanosheets are cut into much smaller GQDs. The concentration of obtained GQD aqueous solution is 5.8 mg mL^{-1} and the yield is 77.3 % which is higher than most previous reports. [27-31] This method is so easy that the reaction liquid can be directly employed for further applied research (such as fluorescent imaging in *vitro*) after simple centrifugal separation without further purification (Figure S3).

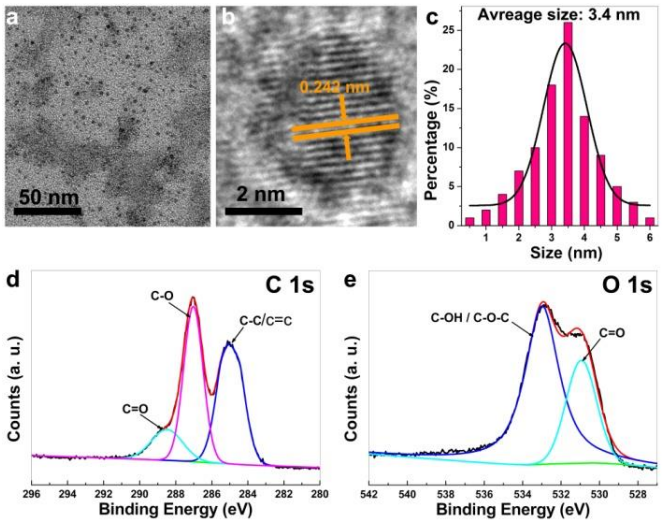

Figure 2 (a) TEM image of GQDs. (b) High resolution TEM image of a single GQD. (c) Corresponding size distribution histogram of GQDs with the black Gaussian fitting curve. (d) C 1s XPS spectrum (e) O 1s XPS spectrum of GQDs.

Transmission electron microscopy (TEM) can provide direct product evidence. There were no large GOs for all the samples. Figure 2a-c shows the typical TEM images and corresponding size distribution of GQDs. Homogeneous dots with a lateral size distribution of 1-6 nm and an average diameter of 3.4 nm were found. The distinct crystal lattice in Figure 2b indicates the crystallinity with the lattice parameter of 0.242 nm, which is the (1120) lattice fringe of graphene. [32] Raman spectrum was shown in Figure S4. The peaks centred at ca. 1368 cm^{-1} and 1384 cm^{-1} are D and G band of sp^2 carbon materials, respectively. The intensity ratio I_D/I_G is 0.61, indicating the good crystalline nature of GQDs. [6, 7]

The X-ray photoelectron spectroscopy (XPS) spectrum was undertaken to probe surface groups of GQDs (Figure 2d and e). The XPS survey spectrum for GQDs shows a C 1s peak at ca. 284.2 eV, along with an O 1s peak at ca. 532 eV (Figure S5). The O/C atomic ratio is 0.36 (the O/C atomic ratio is usually 0.05-0.4 [33]), the high O/C atomic ratio indicates the abundant oxygen-containing function groups in GQDs thus obtained. [34] Figure 2d shows the well-fitted C 1s spectrum which can be divided into three different peaks. The peak located at 284.98 eV, 287.00 eV and 288.49 eV corresponding to the signals of C-C/C=C, C-O and C=O, respectively. [35-40] The O 1s XPS spectrum (Figure 2e) can be divided into two different peaks (Figure 2e), which correspond to the signals of C-OH or C-O-C (533.4 eV) and C=O (532.4 eV). These XPS results indicate that GQDs have abundant periphery carboxylic groups. [41-45] The XPS results were doubly confirmed using Fourier Transform Infrared Spectroscopy (Figure S6). The peak located at 3431, 2918, 1646, 1426 and 1058 cm^{-1} corresponding to the signals of -OH, C=O, C=C, -COO and C-O groups of both GO and GQDs. [46-49] This indicates the similar oxygen-containing function groups of GO and GQDs and corresponding to the XPS results. CH stretching peak of C(=O)-H is located at 2553 cm^{-1}, the increased intensity of CH stretching peak in GQDs indicating the abundant C(=O)-H groups in GQDs. [47] Moreover, these results suggest the obtained GQDs have much more diversified oxygen-containing function groups (C=O and C-O groups) than that of previous reported GQDs. This indicates the different mechanism in our approach. [49] These periphery carboxylic groups passivated the GQDs, which may result in the high quantum yield (ϕ) and good stability.

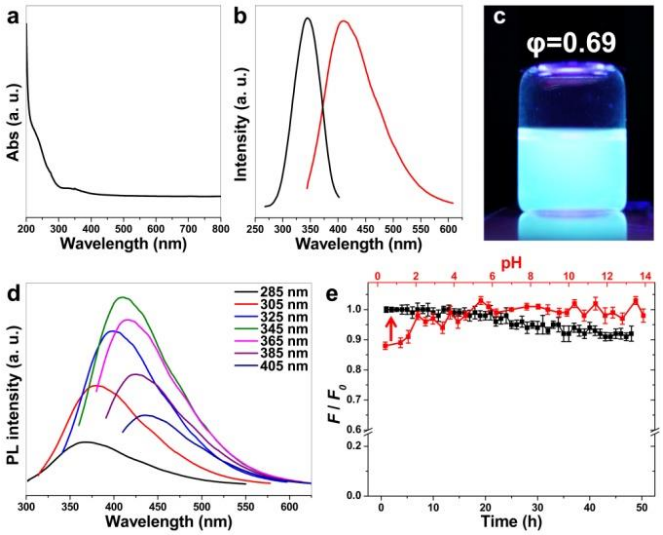

Figure 3 (a) UV-vis absorption spectrum of GQD aqueous solution. (b) Normalized PL (red curve) and PLE (black curve) of GQD aqueous solution. (c) Digital image of GQD aqueous solution (2.0 mg mL^{-1}) under UV-light (centre wavelength 365 nm). (d) PL spectra of GQDs recorded for progressively longer excitation wavelength of 20 nm increments (285-405 nm). (e) Stability of GQDs (0.5 mg mL^{-1}). Red curve: PL intensity change of GQDs under different pH. F_0 and F are PL intensity of GQDs when pH is 7 and corresponding pH, respectively. Black curve: photostability of GQDs under

Journal of Materials Chemistry B Accepted Manuscript

This journal is © The Royal Society of Chemistry 20xx

Please do not adjust margins

365 nm UV light (100 W) at room temperature. The F_0 and F are PL intensity when t=0 and at corresponding times, respectively.

The optical properties of GQDs were studied by UV-vis absorption and PL spectroscopy. The UV-vis absorption spectrum of GQDs (Figure 3a) shows a typical π-π^* transition absorption peak (due to the of aromatic sp^2 domains) around 250 nm, [46] a n-π^* transition absorption peak around 340 nm, [47] and a long tail extending into the visible range. The strong and sharp PL emission peak (λ_{em}) at 408 nm can be observed at an excitation wavelength (λ_{ex}) of 345 nm (red curve in Figure 3b). The full-width at half-maximum (FWHM) of PL peak is 70 nm, which is smaller than previous reports (Table S1). The ϕ is 0.69, which is also higher than most previous reports (Table S1). This can be attributed to the passivation by periphery carboxylic groups. [48] As shown in Figure 3c, the GQD aqueous solution gives bright blue-green PL under UV-light (centre wavelength of UV-light is 365 nm). The Commission International d'Eclairage (Figure S7) chromaticity coordinates for GQDs is (0.16, 0.21). Like other reported GQDs, when the excitation wavelength changes from 285 to 405 nm, the PL peak correspondingly shifts from 365 to 418 nm. This can be due to the abundant periphery carboxylic groups, particle sizes , or different surface state of GQDs. [12, 49-51]

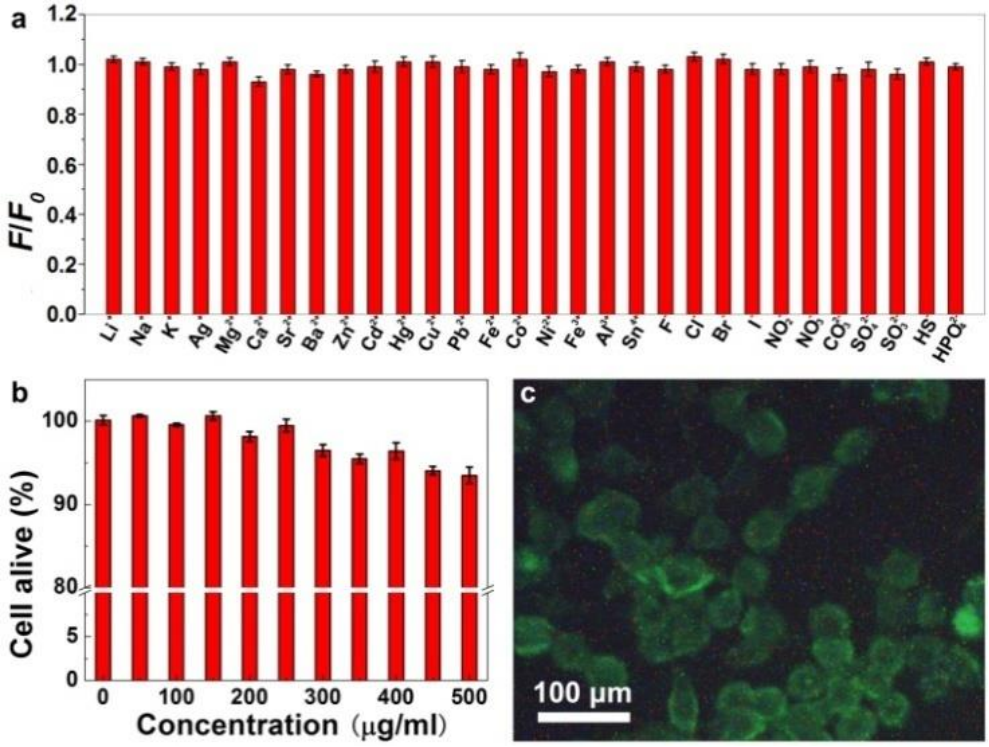

Figure 4 (a) The difference in PL intensity of GQD aqueous solution between the blank and solutions containing different common positive ions and negative ions (F_0 and F are PL intensities in the absence and presence of ions, respectively. The concentrations of all ions are all 0.1 M, the concentrations of GQD is 0.5 mg mL^{-1}). (b) Metabolic activity of HeLa cells treated with different concentrations of GQDs. (c) Confocal fluorescence microphotograph of HeLa cells incubated with 100 μg/mL GQDs (λ_{ex} = 350 nm)

These GQDs showed excellent photo-stability under very hard conditions (Figure 3e). Photostability of GQDs was measured under 365 nm UV-light (100 W) at room temperature. The PL intensity of GQDs shows no change by the UV exposure for 48 h (black curve in Figure 3e). These GQDs also show good stability under visible light irradiation and different pH. No obvious change of PL intensity was observed when the GQD aqueous solution was exposed to visible light irradiation for 15 days (Figure S8) or pH=1-14 (red curve in Figure 3e). What's more, even refluxed in acid (HCl aqueous solution, pH=1) or base (NaOH aqueous solution, pH=13), no obvious change of PL intensity can be observed (Figure S9, 10).

The anti-interference ability is also an important performance of GQDs. Figure 4a shows the anti-interference ability of these GQDs, the GQDs does not give any observable quenching for many common positive ions and negative ions such as: Li^+, Na^+, K^+, Ag^+, Mg^{2+}, Ca^{2+}, Sr^{2+}, Ba^{2+}, Zn^{2+}, Cd^{2+}, Hg^{2+}, Cu^{2+}, Pb^{2+}, Fe^{2+}, Fe^{3+}, Al^{3+}, Sn^{4+}, F^-, Cl^-, Br^-, I^-, NO_2^-, NO_3^-, CO_3^{2-}, SO_4^{2-}, SO_3^{2-}, HPO_4^{2-} and HS^-. These results indicate that these GQDs may be used in fluorescent imaging.

All above results indicate the obtained GQDs have good PL properties, stability and anti-interference ability. This suggests the GQD aqueous solution can be used in fluorescent imaging. Indeed, the GQD aqueous solution obtained after simple centrifugal separation without further purification can be directly employed for fluorescent imaging in *vitro* since there aren't any inorganic salt and acid residues as by-products. To prove it, we tested the in *vitro* cytotoxicity of GQDs using the HeLa cell line first. The metabolic activity of HeLa cells was treated with different concentrations of GQDs (Figure 4b). Varied concentrations of GQDs were added to the cells cultured in 96 well-plates and incubated for 24 h. Subsequently, a standard assay was performed to assess the cell viabilities after the GQDs treatments. No significant reduction in cell viability was observed for cells treated with GQDs even at high concentrations

Journal of Materials Chemistry B Accepted Manuscript

Please do not adjust margins

(up to 500 μg mL^{-1}). Finally, HeLa cells were also used to evaluate the property of the GQDs to assess the prospects of the GQDs as a bio-imaging material. The GQDs were incubated with HeLa cells to show their bio-imaging ability recorded by confocal microscopy (Figure 4c). Bright green PL is observed inside the cells, which means that the GQDs have been internalized by the HeLa cells.

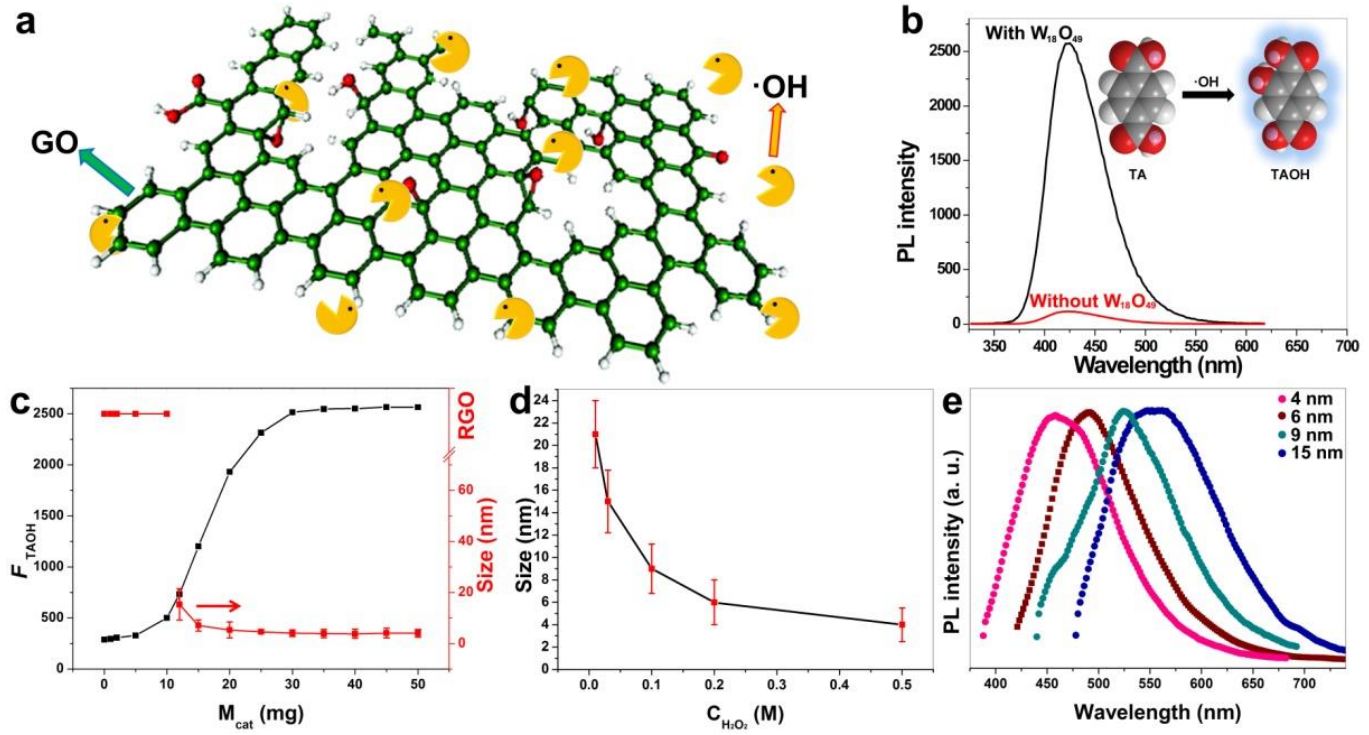

Figure 5 (a) Schematic diagram of oxidize and cut progress. (b) PL spectra of the mixed solution of TA, $W_{18}O_{49}$ and H_2O_2 aqueous solution and only TA, and H_2O_2 after 12 h reaction. The inset is the reaction between ·OH and TA. The concentration of TA in all experiments is 50 mM. (c) Change of ·OH's concentration and GQD lateral size with different dosages of $W_{18}O_{49}$ (GO: 15 mg mL^{-1}, H_2O_2: 1.0 M, TA: 50 mM, volume: 10.0 mL, reaction temperature: 200 °C, reaction time: 72 h). (d) Lateral size of GQDs which obtained under different concentration of H_2O_2 (0.5, 0.2, 0.1, 0.03 and 0.01 M). (e) Normalized PL spectra of different sized GQDs (4, 6, 9 and 15 nm).

Finally, we studied the mechanism, especially the catalyst effect. The possible mechanism is as follows. The $W_{18}O_{49}$ nanowires lead to catalytic decomposition of H_2O_2 into ·OH during the hydrothermal process. The generated ·OH in the mixture has very high reactivity and strong oxidizing property, [4, 20] and it can oxidize and cut the GO sheets effectively (Figure 5a). In order to validate the importance of catalyst, we used only H_2O_2 and GO for the hydrothermal reaction under the same conditions for comparison. Without the catalyst, the reaction product is complicated (Figure S11). The black flotage is the agglomeration of reduced GO nanosheets. The liquid has a shallow colour after filtration to remove the large reduced GO sheets, and its PL is very weak with a quantum yield less than 10%, which is consistent with Ref. 49. We further designed experiments to confirm the actual ·OH concentration in the mixture. The terephthalic acid (TA) was used as a fluorescent probe for ·OH tracking because it could capture ·OH and generate 2-hydroxy terephthalic acid (TAOH), which emits unique fluorescence around 435 nm. [7, 52, 53] The black curve in Figure 5b shows the PL intensity in the mixed solution of TA, $W_{18}O_{49}$ and H_2O_2 aqueous solution after 12 h reaction under 200 °C. Compared with control experiments (TA and H_2O_2 without $W_{18}O_{49}$, red curve in Figure 5b), remarkable PL enhancement at 435 nm indicated that the presence of catalyst is very critical for high concentration ·OH. [42]

We further investigated the possible control on the ·OH concentration based on the catalytic process. As shown in Figure 5c, when the dosage of $W_{18}O_{49}$ is less than 15 mg (in 10mL reaction liquid, mass concentration: 1.5 mg mL^{-1}), the concentration of ·OH is too low to effectively cut GO sheets, and what we get after hydrothermal reaction is reduced GO (RGO) as by-products. When the dosage of $W_{18}O_{49}$ is 15-30 mg (mass concentration: 1.5-3.0 mg mL^{-1}), the concentration of ·OH quickly spiral upwards, and almost all the GO sheets were cut into GQDs without any by-products. Finally, when the dosage of $W_{18}O_{49}$ is 30-50 mg (mass concentration: 3.0-5.0 mg mL^{-1}), both the concentration of ·OH and the lateral size of GQDs became stable. This indicates the appropriate dosage of $W_{18}O_{49}$ is 1.5-5.0 mg mL^{-1}. Another factor for ·OH generation is the H_2O_2 concentration. As shown in Figure 5d, when the concentration of H_2O_2 is 0.5, 0.2, 0.1, 0.03 and 0.01 M, the average diameter of obtained GQDs is 4, 6, 9, 15 and 21 nm, respectively. All these homogeneous GQDs show narrow lateral size distribution. Moreover, the λ_{ex} is red shifted with the increasing of the size, which indicates this method can also obtain the GQDs with tunable λ_{ex} (Table S1). The λ_{ex} of these GQDs is 402, 421, 474 and 498 nm, respectively, as shown in Figure 5e. Moreover, the ϕ of these GQDs is all higher than 45% (Table S1) which indicates the good PL properties of these GQDs.

Journal of Materials Chemistry B Accepted Manuscript

This journal is © The Royal Society of Chemistry 20xx

Please do not adjust margins

Conclusions

In summary, we developed a new mild, clean and high-efficient method for preparation of GQDs without by-products. The ·OH which produced from the catalytic decomposition of H_2O_2 can oxidize and cut all the GO sheets into GQDs. The lateral size of GQDs can be easily controlled by changing the dosages of catalyst and H_2O_2. Moreover, the obtained GQDs show high ϕ and excellent photo-stability. This as-prepared GQD aqueous solution can be directly applied to fluorescent imaging in *vitro*. Our approach is helpful to develop large scale preparation of GQDs and facilitate GQDs' applications.

Acknowledgements

This work was supported by projects from the National Science and Technology Major Project (2011ZX02707), the National Natural Science Foundation of China (61136005), the Chinese Academy of Sciences (KGZD-EW-303), the Jiangsu Province Cultivation base for State Key Laboratory of Photovoltaic Science and Technology (201508), Jiangsu Province Industry-University-Research joint innovation fund (BY2013024-01) , Natural Science Foundation of the Jiangsu Higher Education Institutions of China (14KJA430001).

Notes and references

† *These authors (Chong Zhu and Siwei Yang) contributed equally.*
* *Corresponding author: Prof. Jianning Ding, dingjn@cczu.edu.cn, Prof. Guqiao Ding, gqding@mail.sim.ac.cn.*

1 P. He, J. Sun, S. Y. Tian, S. W. Yang, S. J. Ding, G. Q. Ding, X. M. Xie and M. H. Jiang, *Chem. Mater.*, 2015, **27**, 218.
2 S. W. Yang, J. Sun, X. B. Li, W. Zhou, Z. Y. Wang, P. He, G. Q. Ding, X. M. Xie, Z. H. Kang and M. H. Jiang, *J. Mater. Chem. A*, 2014, **2**, 8660.
3 X. Huang, Z. Yin, S. Wu, X. Qi, Q. He, Q. Zhang, Q. Yan, F. Boey and H. Zhang, *Small*, 2011, **7**, 1876.
4 P. P. Zhang, X. N. Zhao, Y. C. Ji, Z. F. Ouyang, X. Wen, J. F. Li, Z. Q. Su and G. Wei, *J Mater Chem B*, 2015, **3**, 2487.
5 L. A. Ponomarenko, F. Schedin, M. I. Katsnelson, R. Yang, E. W. Hill, K. S. Novoselov and A. K. Geiml, *Science*, 2008, **320**, 356.
6 J. Sun, S. W. Yang, Z. Y. Wang, H. Shen, T. Xu, L. T. Sun, H. Li, W. W. Chen, X. Y. Jiang, G. Q. Ding, Z. H. Kang, X. M. Xie and M. H. Jiang, *Part. Part. Syst. Charact.*, 2015, **32**, 434.
7 S. W. Yang, J. Sun, P. He, X. X. Deng, Z. Y. Wang, C. Y. Hu, G. Q. Ding and X. M. Xie, *Chem. Mater.*, 2015, **27**, 2004.
8 C. K. Chua, Z, Sofer, P. Simek, O. Jankovsky, K. Klimova, S. Bakardjieva, S. H. Kuckova and M. Pumera, *ACS Nano*, 2015, **9**, 2548.
9 X. J. Zhou, Y. Zhang, C. Wang, X. C. Wu, Y. Q. Yang, B. Zheng, H. X. Wu, S. W. Guo and J. Yan, *ACS Nano*, 2012, **6**, 6592.
10 H. J. Sun, N. Gao, K. Dong, J. S. Ren and X. G. Qu, *ACS Nano*, 2014, **8**, 6202.
11 Z. L. Zhu, J. N. Ma, Z. L. Wang, C. Mu, Z. T. Fan, L. L. Du, Y. Bai, L. Z. Fan, H. Yan, D. L. Phillips and S. H. Yang, *J. Am. Chem. Soc.*, 2014, **136**, 3760.
12 Y. Li, Y. Hu, Y. Zhao, G. Q. Shi, L. E. Deng, Y. B. Hou and L. T. Qu, *Adv. Mater.*, 2011, **23**, 776.
13 S. J. Zhu, J. H. Zhang, S. J. Tang, C. Y. Qiao, L. Wang, H. Y. Wang, X. Liu, B. Li, Y. F. Li, W. L. Yu, X. F. Wang, H. C. Sun and B. Yang, *Adv. Funct. Mater.*, 2012, **22**, 4732.
14 J. K. Kim, M. J. Park, S. J. Kim, D. H. Wang, S. P. Cho, S. K. Bae, J. H. Park and B. H. Hong, *Acs Nano*, 2013, **7**, 7207.
15 M. Bacon, S. J. Bradley and T. Nann, *Part. Part. Syst. Charact.*, 2014, **31**, 415.
16 J. Zong, Y. Zhu, X. Yang, J. Shen and C. Li, *Chem. Commun.*, 2011, **47**, 764.
17 R. Q. Ye, C. S. Xiang, J. Lin, Z. W. Peng, K. W. Huang, Z. Yan, N. P. Cook, E. L. G. Samuel, C. C. Hwang, G. D. Ruan, G. Ceriotti, A. R. O. Raji, A. A. Marti and J. M. Tour, *Nat. Commun.*, 2013, **6**, 7063.
18 Y. Li, Y. Hu, Y. Zhao, G. Shi, L. Deng, Y. Hou and L. Qu, *Adv. Mater.*, 2011, **23**, 776.
19 S. Zhu, J. Zhang, X. Liu, B. Li, X. Wang, S. Tang, Q. Meng, Y. Li, C. Shi, R. Hu and B. Yang, *RSC Adv.*, 2012, **2**, 2717.
20 X. J. Zhou, Y. Zhang, C. Wang, X. C. Wu, Y. Q. Yang, B. Zheng, H. X. Wu, S. W. Guo, and J. Y. Zhang, *ACS Nano*, 2012, **6**, 6592–6599.
21 C. Volk, C. Neumann, S. Kazarski, S. Fringes, S. Engels, F. Haupt, A. Muller, and C. Stampfer, *Nat. Commun.*, 2012, **4**, 1753.
22 X. Yan, X. Cui and L. Li, *J. Am. Chem. Soc.*, 2010, **132**, 5944.
23 L. Wang, Y. L. Wang, T. Xu, H. B. Liao, C. J. Yao, Y. Liu, Z. Li, Z. W. Chen, D. Y. Pan, L. T. Sun and M. H. Wu, *Nat. Commun.*, 2015, **5**, 5357.
24 K. Jiang, S. Sun, L. Zhang, Y. Lu, A. G. Wu, C. Z. Cai and H. W. Lin, *Angew. Chem. Int. Ed.*, 2015, **54**, 1.
25 R. L. Liu, D. Q. Wu, X. L. Feng and K. Mullen, *J. Am. Chem. Soc.*, 2011, **133**, 15221.
26 X. Li, S. W. Yang, J. Sun, P. He, X. Xu and G. Ding, *Carbon*, 2014, **78**, 38.
27 H. Zhu, W. Zhang and S. F. Yu, *Nanoscale*, 2013, **5**, 1797.
28 S.W. Yang, S. Huang, D. Liu and F. Liao, *Synth. Met.*, 2012, **162**, 2228.
29 J. Lee, K. Kim, W. I. Park, B. H. Kim, J. H. Park, T. H. Kim, S. Bong, C. H. Kim, G. Chae, M. Jun, Y. Hwang, Y. S. Jung and S. Jeon, *Nano Lett.*, 2012, **12**, 6078.
30 S. W. Yang, C. Ye, X. Song, L. He and F. Liao, *RSC Adv.*, 2014, **4**, 54810.
31 W. Kwon, Y. H. Kim, C. L. Lee, M. Lee, H. C. Choi, T. W. Lee and S. W. Rhee, *Nano Lett.*, 2014, **14**, 1306.
32 S. W. Yang, C. Zhu, J. Sun, P. He, N. Yuan, J. Ding, G. Ding and X. Xie, *RSC Adv.*, 2015, **5**, 33347.
33 D. Wang, J. F. Chen and L. M. Dai, *Part. Part. Syst. Charact.*, 2015, **32**, 515.
34 Z. H. Zhang, S. J. Xu and P. Y. Wu, *Part. Part. Syst. Charact.*, 2015, **32**, 176.
35 P. Atienzar, A. Primo, C. Lavorato, R. Molinari and H. García, *Langmuir*, 2013, **29**, 6141.
36 T. Zhang, S. W. Yang, J. Sun, X. Li, L. He, S. Yan, X. Kang, C. Hu and F. Liao, *Synth. Met.*, 2013, **181**, 86.
37 G. S. Kumar, R. Roy, D. Sen, U. K. Ghorai, R. Thapa, N. Mazumder, S. Saha and K. K. Chattopadhyay, *Nanoscale*, 2014, **6**, 3384.
38 F. Liao, S. W. Yang, X. Li, L. Yang, Z. Xie, C. Hu, S. Yan, T. Ren and Z. Liu, *Synth. Met.*, 2014, **189**, 126.
39 S. Bayram and L. Halaoui, *Part. Part. Syst. Charact.*, 2013, **30**, 706.
40 S. Yan, S. W. Yang, L. He, C. Ye, X. Song and F. Liao, *Synth. Met.*, 2014, **198**, 142.
41 L. Li, G. Wu, G. Yang, J. Peng, J. Zhao and J. J. Zhu, *Nanoscale*, 2013, **5**, 4015.
42 T. S. Sreeprasad, A. A. Rodriguez, J. Colston, A. Graham, E. Shishkin, V. Pallem and V. Berry, *Nano Lett.*, 2013, **13**, 1757.
43 F. Liao and S. W. Yang, *Synth. Met.*, 2015, **205**, 32.

Journal of Materials Chemistry B Accepted Manuscript

Please do not adjust margins

44 M. Bacon, S. J. Bradley and T. Nann, *Part. Part. Syst. Charact.*, 2014, **31**, 415.
45 H. R. Barzegar, C. Larsen, L. Edman and T. Wågberg, *Part. Part. Syst. Charact.*, 2013, **30**, 715.
46 Y. Dai, H. Long, X. Wang, Y. Wang, Q. Gu, W. Jiang, Y. Wang, C. Li, T. H. Zeng, Y. Sun and J. Zeng, *Part. Part. Syst. Charact.*, 2014, **31**, 597.
47 R. Gokhale and P. Singh, *Part. Part. Syst. Charact.*, 2014, **31**, 433.
48 H. L. Dong, M. Roming and C. Feldmann, *Part. Part. Syst. Charact.*, 2015, **32**, 467.
49 X. Zhu, X. Xiao, X. Zuo, Y. Liang and J. Nan, *Part. Part. Syst. Charact.*, 2014, **31**, 801.
50 Y. Li, Y. Zhao, H. Cheng, Y. Hu, G. Shi, L. Dai, L. Qu, *J. Am. Chem. Soc.*, 2012, **134**, 15.
51 L. Tang, R. Ji, X. Cao, J. Lin, H. Jiang, X. Li, K. S. Teng, C. M. Luk, S. Zeng, J. Hao, S. P. Lau, *ACS Nano*, 2012, **6**, 5102.
52 F. Liao, X. Song, S. Yang, C. Hu, L. He, S. Yan and G. Ding, *J. Mater. Chem. A*, 2015, **3**, 7568.
53 K. Ishibashi, A. Fujishima, T. Watanabe and K. Hashimoto, *Electrochem. Commun.*, 2000, **2**, 207.

Journal of Materials Chemistry B Accepted Manuscript

This journal is © The Royal Society of Chemistry 20xx

Please do not adjust margins